This article has been accepted for publication in a future issue of this journal, but has not been fully edited. Content may change prior to final publication.
Citation information: DOI: 10.1109/JIOT.2025.3608094, EEE Internet of Things Journal

PID Containment Control for Multi-Agent Systems With Multi-Rate Measurements Under Sensor Resolution Constraints

Yezheng Wang, Zidong Wang, Lei Zou, Fan Wang, and Hongli Dong

***Abstract*—This paper investigates the proportional-integral-derivative (PID) containment control problem for a class of linear multi-agent systems with multi-rate measurements under the constraint of sensor resolution. The sensors of agents are classified into two distinct groups, characterized by their relatively fast and slow sampling periods. The concept of sensor resolution is introduced to quantify the ability of sensors to detect the smallest changes in information. A PID controller with an improved structure is proposed to achieve containment control, ensuring that follower agents remain within the convex hull formed by the leader agents. The closed-loop system is reformulated into a simplified representation, incorporating both sampling characteristics and communication topology. Sufficient conditions are then derived to guarantee the exponentially ultimate boundedness of the tracking error. Based on these conditions, an iterative algorithm is developed for computing the required controller gains. Finally, a simulation study, along with comparative analyses, is conducted to validate the effectiveness of the proposed approach.**

***Index Terms*—Multi-agent systems, sensor resolution, multi-rate measurements, proportional-integral-derivative (PID) control, containment control.**

I. Introduction

A multi-agent system (MAS) is a framework in which multiple intelligent agents interact within a shared environment to achieve designated objectives. In recent decades, the cooperative challenges associated with MASs have been extensively studied due to their wide-ranging applications in unmanned aerial vehicles, multi-robot systems, distributed sensor networks, and other domains. In practical engineering contexts, typical cooperative behaviors include consensus, formation, containment, and tracking [4], [5], [15], [18], [19], [37], [44]. These behaviors have attracted considerable research attention from both practitioners and theorists. In MAS research, key considerations involve the utilization of communication topology and the associated computational overhead, both of which have a significant impact on the feasibility and effectiveness of the implemented control protocols.

The containment control problem, recognized as a critical issue in the study of MASs, has attracted significant research interest in recent years. Containment refers to the process of driving all followers into a specific geometric region, typically a convex hull, which is defined by the leaders under a designed control protocol. This concept possesses substantial practical significance, particularly in applications involving obstacle avoidance. A foundational study on containment control has been presented in [16], where a hybrid "stop-go" policy has been employed to ensure that the followers remain within a predetermined constrained area for safety. Subsequent research has extensively investigated containment problems across various MAS configurations, contributing to a substantial body of literature [8], [9], [20], [40]. For instance, in [6], a distributed containment control approach has been proposed for double-integrator MASs. Furthermore, in [7], an event-based containment protocol has been developed for general linear MASs, where a boundedness index has been introduced to evaluate containment performance.

In practical scenarios, obtaining complete state information of MASs is notably challenging, primarily due to limitations in measurement capabilities. Consequently, either relative or absolute sensor measurements are commonly leveraged for control purposes. A prevalent assumption in the literature is that the sampling periods of various sensors are identical, which simplifies theoretical analysis [21], [23], [27], [31], [32], [38], [42], [46], [47]. However, this assumption does not always hold for MASs with complex dynamics, as the sampling periods often depend on the types of sensors employed. In MASs, different sensors are typically utilized to measure distinct signals, resulting in a multi-rate phenomenon. For instance, in mobile robotics, global positioning systems, which operate at a relatively low sampling frequency, are used for positional detection, whereas speed transmitters, which have a higher sampling frequency, are employed to meet real-time requirements. This disparity in sensor sampling rates intro-

This work was supported in part by the National Natural Science Foundation of China under Grants 61933007, 62273087, and U21A2019, the Startup Foundation for Introducing Talent of Nanjing University of Information Science and Technology under Grants 1083142501018, and 1083142401006, the Hainan Province Science and Technology Special Fund under Grant ZDYF2022SHFZ105, the Royal Society of the UK, and the Alexander von Humboldt Foundation of Germany. *(Corresponding author: Zidong Wang.)*

Yezheng Wang and Fan Wang are with the School of Automation, Nanjing University of Information Science and Technology, Nanjing 210044, China. (Emails: wangyz_sdust@163.com; wangfan.92128@gmail.com).

Zidong Wang is with the College of Electrical Engineering and Automation, Shandong University of Science and Technology, Qingdao 266590, China; and is also with the Department of Computer Science, Brunel University London, Uxbridge, Middlesex, UB8 3PH, United Kingdom. (Email: Zidong.Wang@brunel.ac.uk).

Lei Zou is with the College of Information Science and Technology, Donghua University, Shanghai 201620, China; and is also with the Engineering Research Center of Digitalized Textile and Fashion Technology, Ministry of Education, Shanghai 201620, China. (Email: zouleicup@gmail.com).

Hongli Dong is with the State Key Laboratory of Continental Shale Oil, Northeast Petroleum University, Daqing 163318, China; is also with the Artificial Intelligence Energy Research Institute, Northeast Petroleum University, Daqing 163318, China; and is also with the Heilongjiang Provincial Key Laboratory of Networking and Intelligent Control, Northeast Petroleum University, Daqing 163318, China. (Email: shiningdhl@vip.126.com).

Citation information: DOI: 10.1109/JIOT.2025.3608094, EEE Internet of Things Journal

duces diverse time scales within the system, posing significant challenges for system analysis and controller design. Recent advancements have led to the development of several effective methods for addressing these multi-rate phenomena in both centralized and distributed systems [1], [10], [11], [22], [35], [43].

In addition to sampling frequency, resolution constitutes a critical parameter of sensors, as it quantifies their ability to detect the smallest variations in measurements [17], [29], [30]. Sensors with low resolution exhibit reduced sensitivity to changes in the target, leading to substantial deviations from actual values. If not properly addressed, measurement errors induced by insufficient resolution can significantly degrade both estimation and control performance. Current research on sensor resolution primarily focuses on resolution modeling and the associated filtering challenges. For instance, in [2] and [3], tracking issues arising from erroneous measurements due to sensor resolution have been investigated in the context of multiple maneuvering targets. Additionally, in [35], a recursive state estimator has been developed for time-varying systems, with full consideration of resolution effects.

In the domain of control theory, proportional-integral-derivative (PID) control is recognized as one of the most established methodologies, with its origins traceable to the 1930s. Despite the emergence of numerous advanced control strategies over the decades, PID control continues to be widely utilized in contemporary industrial applications. This enduring relevance can be attributed to its advantages, including clear physical interpretation, significant robustness, and ease of tuning [12]–[14], [39]. The PID control technique has been demonstrated to be effective in handling system complexities such as uncertainties and time delays and is extensively applied to stabilization, tracking, optimization, and performance enhancement tasks in various complex systems. Recent advancements in MASs have led to investigations into PID-based cooperative control. For instance, in [24] and [25], PID-based approaches have been examined for tracking problems, addressing challenges related to communication delays and uncertainties. Additional representative studies on this topic can be found in [26], [28], [34], [36], [45].

By reviewing the literature on the relevant engineering complexities, the following observations have been made. 1) Regarding sensor resolution, the majority of existing research has focused on mathematical modeling and filtering issues [2], [3], [35], while comparatively limited attention has been given to control problems, particularly in the context of distributed control. 2) With respect to MASs, PID-like control strategies have primarily been developed for tracking or consensus tasks, whereas the problem of PID-based containment control under the combined constraints of multi-rate sampling and sensor resolution remains largely unexplored. These identified gaps in the existing body of knowledge serve as the motivation for the present study.

Based on the above discussions, the bounded PID containment control problem is examined by assessing the impacts of sensor resolution and multi-rate sampling on system performance. The objective is to understand how these factors influence the stability, accuracy, and responsiveness of MASs under practical constraints. The key challenges addressed in this study are as follows: 1) analyzing how sensor resolution and multi-rate sampling affect the overall performance of MASs, particularly in terms of stability, transient response, and steady-state accuracy; 2) developing a viable and computationally efficient algorithm for determining PID controller gains that ensure effective containment control, and the proposed approach must account for constraints imposed by heterogeneous sampling rates and resolution limitations while maintaining robustness against uncertainties; and 3) exploring adaptive tuning mechanisms to dynamically adjust control parameters in response to changing sensor characteristics, ensuring that variations in measurement precision and sampling intervals do not degrade system performance.

In response to the identified challenges, the main contributions of this paper are summarized as follows.

1) The PID containment control problem is, for the first time, investigated for general linear MASs consisting of multiple leaders and followers. A comprehensive measurement model is established to encapsulate the combined effects of multi-rate sampling and sensor resolution, providing a more realistic representation of practical systems.
2) A novel variable transformation technique is introduced to derive a concise system model. Based on this formulation, sufficient conditions are established to ensure the boundedness of the tracking error systems, offering theoretical guarantees for stability and performance.
3) By leveraging the underlying topological structure, an iterative algorithm is developed for computing the PID controller gains while simultaneously optimizing relevant index parameters. The proposed method is designed to be independent of the total number of agents in the MAS, ensuring scalability and applicability to large-scale systems.

The remainder of this paper is organized as follows. Section II provides a description of the fundamental problem, including the system, measurement, and controller models, along with a detailed explanation of the control objectives. Section III presents the main results on boundedness analysis and controller design. In Section IV, a numerical example is provided to validate the effectiveness of the proposed method. Finally, Section V concludes the paper.

II. Problem Statement and Preliminaries

A. Preliminaries

In this paper, we consider a class of MASs composed of R ($R \in \mathbb{N}_+$) agents in which W ($W \in \mathbb{N}_+,\ W < R$) agents function as followers and the remaining $R - W$ agents act as leaders. Without loss of generality, we use indices $1, 2, \cdots, W$ to represent followers, and $W+1, W+2, \cdots, R$ to denote leaders. For such a system, agents exchange information according to a fixed topology, represented by an undirected graph $\mathcal{G} \triangleq \{\mathbb{V}, \mathbb{E}, \mathcal{A}\}$, where $\mathbb{V} \triangleq \{1, 2, \cdots, R\}$ is the node set; $\mathbb{E} \triangleq \{(i_1, j_1), (i_2, j_2), \cdots\} \in \{(i,j) | i, j = 1, 2, \cdots, R\}$ is the edge set; and $\mathcal{A} \triangleq [a_{i,j}]_{i,j=1,\cdots,R}$ corresponds to the weighted adjacency matrix with non-negative elements.

This article has been accepted for publication in a future issue of this journal, but has not been fully edited. Content may change prior to final publication.
Citation information: DOI: 10.1109/JIOT.2025.3608094, EEE Internet of Things Journal

A positive weight $a_{i,j} > 0$ signifies that: 1) agent i can receive the information from agent j; 2) agent j is a neighbor of agent i; and 3) $(j,i) \in \mathbb{E}$. Here, self-edges are not allowed, i.e., $(i,i) \notin \mathbb{E}$ for $\forall i \in \mathbb{V}$. The set of all neighbors of agent i is defined as $\mathcal{N}_i \triangleq \{j|(j,i) \in \mathbb{E}\}$. An agent is classified as a leader if it has no neighbors; otherwise, it is designated as a follower. Define the in-degree of agent i as $d_i \triangleq \sum_{j\in\mathcal{N}_i} a_{i,j}$ with $\mathcal{D} \triangleq \mathrm{diag}\{d_1, d_2, \cdots, d_R\}$. Then, an auxiliary topological matrix is defined as $L \triangleq \mathcal{A} - \mathcal{D}$.

Since the $R-W$ leaders have no neighbors, the matrix L in this paper has the following specific form:

$$L = \begin{bmatrix} L_1 & L_2 \\ 0_{(R-W)\times W} & 0_{(R-W)\times(R-W)} \end{bmatrix}$$

where $L_1 \in \mathbb{R}^{W\times W}$ and $L_2 \in \mathbb{R}^{W\times(R-W)}$.

Regarding the topology of the considered MASs, the following assumption, lemma, and definition are presented.

Assumption 1: [7] For each follower, at least one leader has a directed path to that follower.

Lemma 1: [7] Under Assumption 1, the matrix L_1 is negative definite. Furthermore, the matrix $-L_1^{-1}L_2$ is nonnegative and the sum of each row equals one.

Definition 1: [7] For a set of points of $\mathbb{H} \triangleq \{h_1, h_2, \cdots, h_\tau\}$, its convex hull $\mathrm{Co}(\mathbb{H})$ is defined as

$$\mathrm{Co}(\mathbb{H}) \triangleq \left\{ \sum_{\iota=1}^{\tau} \beta_\iota h_\iota \middle| h_\iota \in \mathbb{H}, \beta_\iota \geq 0, \sum_{\iota=1}^{\tau} \beta_\iota = 1 \right\}.$$

To facilitate the subsequent discussion, two sets associated with followers and leaders are defined as follows:

$$\mathbb{F} \triangleq \{1, 2, \cdots, W\}, \quad \mathbb{L} \triangleq \{W+1, W+2, \cdots, R\}.$$

B. System Model

Consider the following linear homogeneous MASs:

$$\begin{cases} x_i(T_{n+1}) = Ax_i(T_n) + Bu_i(T_n) + E\omega_i(T_n), & i \in \mathbb{F}, \\ x_j(T_{n+1}) = Ax_j(T_n) + E\omega_j(T_n), & j \in \mathbb{L} \end{cases} \tag{1}$$

where T_n is the n-th update instant of states. For the i-th agent, $x_i(T_n) \in \mathbb{R}^{o_x}$ is the state variable; $u_i(T_n) \in \mathbb{R}^{o_u}$ is the control input; $\omega_i(T_n) \in \mathbb{R}^{o_\omega}$ is an amplitude-bounded noise term satisfying $\omega_i^T(T_n)\omega_i(T_n) \leq \hat{\omega}_i$ with $\hat{\omega}_i > 0$ being a known scalar; o_x, o_u, o_ω are known positive integers; and A, B, E are known constant matrices.

Remark 1: The linear homogeneous MASs (1) provide a versatile framework for modeling a wide range of large-scale engineering systems, including generic vehicles, autonomous mobile robots, and quadrotor systems. Owing to their model simplicity and broad applicability, such systems have been extensively studied in the literature.

For each agent, the employed sensors operate with different sampling periods. The ideal multi-rate measurements (without considering sensor resolution) are modeled as follows [48]:

$$\begin{cases} y_i^f(T_n) = C^f x_i(T_n) + F^f \omega_i(T_n), \\ y_i^s(t_n) = C^s x_i(t_n) + F^s \omega_i(t_n) \end{cases} \tag{2}$$

where the superscript "f" means the fast-sampling-related terms, and the subscript "s" means the slow-sampling-related terms; $y_i^f(T_n) \in \mathbb{R}^{o_{y1}}$ is the output with a relatively fast sampling frequency, while $y_i^s(t_n) \in \mathbb{R}^{o_{y2}}$ is the output with a relatively slow sampling frequency; t_n is the n-th slow sampling instant; and C^f, C^s, F^f and F^s are known matrices with proper dimensions.

Assumption 2: [48] The period of slow sampling is m ($m \in \mathbb{N}_+$) times the period of fast sampling, i.e., $t_{n+1} - t_n = m(T_{n+1} - T_n)$. In addition, the initial sampling instant of sensors is the same, i,e., $t_0 = T_0 = 0$.

Definition 2: [35] Define $y_{i,q}(\cdot)$ as the q-th element of the i-th agent's measurement. If $y_{i,q}(\cdot)$ takes values in the set $\{\kappa r_q | r_q > 0, \kappa = 0, \pm 1, \pm 2, \cdots, \pm\epsilon\}$ with ϵ being a given positive integer, then r_q is called the resolution of the corresponding sensor.

By taking the sensor resolution into account, for the original measurement outputs $y_i^\star(T_n)$, the actual measurements are given as follows:

$$\tilde{y}_{i,q}^\star(T_n) = \begin{cases} \left\lfloor \dfrac{y_{i,q}^\star(T_n)}{r_q^\star} \right\rfloor r_q^\star, & y_{i,q}^\star(T_n) \geq r_q^\star \\ 0, & -r_q^\star < y_{i,q}^\star(T_n) < r_q^\star \\ \left\lceil \dfrac{y_{i,q}^\star(T_n)}{r_q^\star} \right\rceil r_q^\star, & y_{i,q}^\star(T_n) \leq -r_q^\star \end{cases} \tag{3}$$

where the superscript "$\star = f$" denotes the fast-sampling-related variables or parameters, and the superscript "$\star = s$" denotes the slow-sampling-related variables or parameters. Specifically, for $q = 1, 2, \cdots, o_{y_1}$ and $\iota = 1, 2, \cdots, o_{y_2}$, $y_{i,q}^f(T_n)$ is the q-th element of $y_i^f(T_n)$ and $y_{i,\iota}^s(t_n)$ is the ι-th element of $y_i^s(t_n)$; r_q^f and r_ι^s are known scalars. In formula (3), the resolution level of each sensor in two groups with different sampling rates is allowed to be diverse, which is effective in representing the complex sampling cases in reality.

Define the following resolution-introduced output difference:

$$\begin{cases} \Delta_{i,q}^f(T_n) \triangleq \tilde{y}_{i,q}^f(T_n) - y_{i,q}^f(T_n), \\ \Delta_{i,\iota}^s(t_n) \triangleq \tilde{y}_{i,\iota}^s(t_n) - y_{i,\iota}^s(t_n). \end{cases} \tag{4}$$

Then, one has

$$\begin{cases} \tilde{y}_{i,q}^f(T_n) = y_{i,q}^f(T_n) + \Delta_{i,q}^f(T_n), \\ \tilde{y}_{i,\iota}^s(t_n) = y_{i,\iota}^s(t_n) + \Delta_{i,\iota}^s(t_n). \end{cases}$$

We further define the following augmentation vector:

$$\tilde{y}_i^f(T_n) \triangleq \begin{bmatrix} \tilde{y}_{i,1}^f(T_n) \\ \tilde{y}_{i,2}^f(T_n) \\ \vdots \\ \tilde{y}_{i,o_{y_1}}^f(T_n) \end{bmatrix}, \quad \tilde{y}_i^s(t_n) \triangleq \begin{bmatrix} \tilde{y}_{i,1}^s(t_n) \\ \tilde{y}_{i,2}^s(t_n) \\ \vdots \\ \tilde{y}_{i,o_{y_2}}^s(t_n) \end{bmatrix},$$

$$\Delta_i^f(T_n) \triangleq \begin{bmatrix} \Delta_{i,1}^f(T_n) \\ \Delta_{i,2}^f(T_n) \\ \vdots \\ \Delta_{i,o_{y_1}}^f(T_n) \end{bmatrix}, \quad \Delta_i^s(t_n) \triangleq \begin{bmatrix} \Delta_{i,1}^s(t_n) \\ \Delta_{i,2}^s(t_n) \\ \vdots \\ \Delta_{i,o_{y_2}}^s(t_n) \end{bmatrix}.$$

This article has been accepted for publication in a future issue of this journal, but has not been fully edited. Content may change prior to final publication.
Citation information: DOI: 10.1109/JIOT.2025.3608094, EEE Internet of Things Journal

For notation convenience, let $n \triangleq T_n$ and denote $\tilde{y}_i(n)$ as the overall output of agent i ($i \in \mathbb{V}$) under resolution effects. According to Assumption 2, we have

$$\tilde{y}_i(n) = \begin{cases} \begin{bmatrix} \tilde{y}_i^f(n) \\ \tilde{y}_i^s(n) \end{bmatrix}, & \text{if } \operatorname{mod}(n,m) = 0 \\ \begin{bmatrix} \tilde{y}_i^f(n) \\ 0 \end{bmatrix}, & \text{if } \operatorname{mod}(n,m) \neq 0. \end{cases} \tag{5}$$

Note that the multi-rate measurement introduces a switching phenomenon in (5). By introducing the following binary switching variable:

$$\theta(n) \triangleq \begin{cases} 1, & \text{if } \operatorname{mod}(n,m) = 0 \\ 0, & \text{if } \operatorname{mod}(n,m) \neq 0, \end{cases} \tag{6}$$

and considering (2)-(5) simultaneously, we obtain

$$\tilde{y}_i(n) = \bar{C}_{\theta(n)} x_i(n) + \bar{F}_{\theta(n)} \omega_i(n) + \Delta_{i,\theta(n)}(n) \tag{7}$$

where

$$\bar{C}_1 \triangleq \begin{bmatrix} C^f \\ C^s \end{bmatrix}, \quad \bar{C}_0 \triangleq \begin{bmatrix} C^f \\ 0 \end{bmatrix}, \quad \bar{F}_1 \triangleq \begin{bmatrix} F^f \\ F^s \end{bmatrix},$$
$$\bar{F}_0 \triangleq \begin{bmatrix} F^f \\ 0 \end{bmatrix}, \quad \Delta_{i,1}(n) \triangleq \begin{bmatrix} \Delta_i^f(n) \\ \Delta_i^s(n) \end{bmatrix}, \quad \Delta_{i,0}(n) \triangleq \begin{bmatrix} \Delta_i^f(n) \\ 0 \end{bmatrix}.$$

One can infer from Assumption 2 that $\theta(n)$ is deterministic and known, which facilitates the construct of the sampling-dependent controller.

The containment control problem presents considerable challenges due to its inherent multiple constraints. To streamline subsequent analysis, we define the following virtual reference trajectory:

$$x^*(n) \triangleq \left(-L_1^{-1} L_2 \otimes I_{o_x}\right) x^b(n)$$

where

$$x^b(n) \triangleq \begin{bmatrix} x_{W+1}^T(n) & x_{W+2}^T(n) & \cdots & x_R^T(n) \end{bmatrix}^T.$$

According to Lemma 1 and Definition 1, this virtual trajectory constitutes a convex hull spanned by the leader agents $W+1, W+2, \cdots, R$. Consequently, the containment control objective can be equivalently reformulated as a tracking problem, wherein all follower agents are required to converge to $x^*(n)$ while satisfying prescribed performance constraints. This transformation enables the evaluation of containment control performance through the analysis of the tracking error with respect to the virtual reference trajectory.

C. PID Controller

To achieve the desired tracking task, the following PID containment controller is constructed for agent i ($i \in \mathbb{F}$):

$$\begin{aligned} u_i(n) = {} & K_{P,\theta(n)} \sum_{j \in \mathcal{N}_i} a_{i,j} e_{i,j}(n) \\ & + K_{I,\theta(n)} \sum_{j \in \mathcal{N}_i} a_{i,j} \sum_{\sigma=1}^{\bar{\sigma}} e_{i,j}(n-\sigma) \\ & + K_{D,\theta(n)} \sum_{j \in \mathcal{N}_i} a_{i,j} \left(e_{i,j}(n) - e_{i,j}(n-1)\right) \end{aligned} \tag{8}$$

where $e_{i,j}(n) \triangleq \tilde{y}_j(n) - \tilde{y}_i(n)$ and $K_{P,\theta(n)}$, $K_{I,\theta(n)}$, $K_{D,\theta(n)} \in \mathbb{R}^{o_u \times o_y}$ ($o_y \triangleq o_{y_1} + o_{y_2}$) are control gains to be designed.

Remark 2: In the proposed PID controller (8), the error between the measurements of agents and their neighbors is utilized to generate control laws, with the objective of achieving containment. Specifically, the controller gains are designed to be dependent on the switching signal $\theta(n)$, enhancing the flexibility of the design. Moreover, the integral (accumulative) term is constructed based on a fixed time window to reduce the computational and storage burden on agents. As compared to the traditional PID controller, the proposed one enjoys more design degrees of freedom and is thus more effective in controlling large-sale MASs under multiple constraints.

Denoting the following augmentation vector:

$$x^a(n) \triangleq \begin{bmatrix} x_1^T(n) & x_2^T(n) & \cdots & x_W^T(n) \end{bmatrix}^T,$$

one obtains the closed-loop system as follows:

$$\begin{aligned} x^a(n+1) = {} & \left(I_W \otimes A + L_1 \otimes B\bar{K}_{\theta(n)}\bar{C}_{\theta(n)}\right) x^a(n) \\ & + L_2 \otimes B\bar{K}_{\theta(n)}\bar{C}_{\theta(n)} x^b(n) \\ & + \bar{L} \otimes B\bar{K}_{\theta(n)}\bar{F}_{\theta(n)}\omega(n) \\ & + \bar{L} \otimes B\bar{K}_{\theta(n)}\Delta_{\theta(n)}(n) + I_W \otimes E\omega^a(n) \\ & + \sum_{\sigma=1}^{\bar{\sigma}} L_1 \otimes B\tilde{K}_{\sigma,\theta(n)}\bar{C}_{\theta(n-\sigma)} x^a(k-\sigma) \\ & + \sum_{\sigma=1}^{\bar{\sigma}} L_2 \otimes B\tilde{K}_{\sigma,\theta(n)}\bar{C}_{\theta(n-\sigma)} x^b(k-\sigma) \\ & + \sum_{\sigma=1}^{\bar{\sigma}} \bar{L} \otimes B\tilde{K}_{\sigma,\theta(n)}\bar{F}_{\theta(n-\sigma)}\omega(n-\sigma) \\ & + \sum_{\sigma=1}^{\bar{\sigma}} \bar{L} \otimes B\tilde{K}_{\sigma,\theta(n)}\Delta_{\theta(n-\sigma)}(n-\sigma) \end{aligned} \tag{9}$$

and

$$x^b(n+1) = \left(I_{R-W} \otimes A\right) x^b(n) + \left(I_{R-W} \otimes E\right)\omega^b(n) \tag{10}$$

where

$$\bar{K}_{\theta(n)} \triangleq K_{P,\theta(n)} + K_{D,\theta(n)}, \quad \bar{L} \triangleq \begin{bmatrix} L_1 & L_2 \end{bmatrix},$$
$$\tilde{K}_{1,\theta(n)} \triangleq K_{I,\theta(n)} - K_{D,\theta(n)}, \quad \omega(n) \triangleq \begin{bmatrix} \omega^a(n) \\ \omega^b(n) \end{bmatrix},$$
$$\tilde{K}_{2,\theta(n)} = \tilde{K}_{3,\theta(n)} = \cdots = \tilde{K}_{\bar{\sigma},\theta(n)} \triangleq K_{I,\theta(n)},$$
$$\omega^a(n) \triangleq \begin{bmatrix} \omega_1(n) \\ \omega_2(n) \\ \vdots \\ \omega_W(n) \end{bmatrix}, \quad \omega^b(n) \triangleq \begin{bmatrix} \omega_{W+1}(n) \\ \omega_{W+2}(n) \\ \vdots \\ \omega_R(n) \end{bmatrix},$$
$$\Delta_1(n) \triangleq \begin{bmatrix} \Delta_{1,1}(n) \\ \Delta_{2,1}(n) \\ \vdots \\ \Delta_{R,1}(n) \end{bmatrix}, \quad \Delta_0(n) \triangleq \begin{bmatrix} \Delta_{1,0}(n) \\ \Delta_{2,0}(n) \\ \vdots \\ \Delta_{R,0}(n) \end{bmatrix}.$$

Define the tracking error of states by

$$\bar{x}(n) \triangleq x^a(n) - \left(-L_1^{-1} L_2 \otimes I_{o_x}\right) x^b(n).$$

Then, based on (9)–(10), we obtain the tracking error system as follows:

$$\begin{aligned}\bar{x}(n+1) = &\left(I_W \otimes A + L_1 \otimes B\bar{K}_{\theta(n)}\bar{C}_{\theta(n)}\right)\bar{x}(n)\\ &+\sum_{\sigma=1}^{\bar{\sigma}} L_1 \otimes B\tilde{K}_{\sigma,\theta(n)}\bar{C}_{\theta(n-\sigma)}\bar{x}(n-\sigma)\\ &+\left(\bar{L}\otimes B\bar{K}_{\theta(n)}\bar{F}_{\theta(n)} + (I_W\otimes E)\tilde{L}\right)\omega(n)\\ &+\sum_{\sigma=1}^{\bar{\sigma}}\bar{L}\otimes B\tilde{K}_{\sigma,\theta(n)}\bar{F}_{\theta(n-\sigma)}\omega(n-\sigma)\\ &+\bar{L}\otimes B\bar{K}_{\theta(n)}\Delta_{\theta(n)}(n)\\ &+\sum_{\sigma=1}^{\bar{\sigma}}\bar{L}\otimes B\tilde{K}_{\sigma,\theta(n)}\Delta_{\theta(n-\sigma)}(n-\sigma) \quad (11)\end{aligned}$$

where

$$\begin{aligned}\tilde{L} \triangleq &\begin{bmatrix} I_{Wo_\omega} & 0_{Wo_\omega\times(R-W)o_\omega}\end{bmatrix}\\ &+ L_1^{-1}L_2\begin{bmatrix}0_{(R-W)\times W} & I_{(R-W)}\end{bmatrix}\otimes I_{o_x}.\end{aligned}$$

Due to the complex coupling terms in (11), analyzing the dynamics of the error system is highly challenging. To facilitate the theoretical derivation, system (11) is first transformed into a more concise form.

From the topological structure and the definition of matrix L, it is known that L_1 is a symmetric and negative definite matrix. Thus, there exists a matrix $M \in \mathcal{R}^{W\times W}$ (satisfying $M^TM = I$) such that

$$M^TL_1M = \text{diag}\{\lambda_1, \lambda_2, \cdots, \lambda_W\} \triangleq \Theta$$

where $0 > \lambda_1 \geq \lambda_2 \geq \cdots \geq \lambda_W$ are eigenvalues of matrix L_1. Then, by defining $\xi(n) \triangleq (M^T \otimes I_{o_x})\bar{x}(n)$, system (11) is transformed into the following form:

$$\begin{aligned}\xi(n+1) = &\left(I_W\otimes A + \Theta\otimes B\bar{K}_{\theta(n)}\bar{C}_{\theta(n)}\right)\xi(n)\\ &+\sum_{\sigma=1}^{\bar{\sigma}}\left(\Theta\otimes B\tilde{K}_{\sigma,\theta(n)}\bar{C}_{\theta(n-\sigma)}\right)\xi(n-\sigma)\\ &+\left(I_W\otimes B\bar{K}_{\theta(n)}\bar{F}_{\theta(n)}\right)\bar{\omega}(n) + (I_W\otimes E)\tilde{\omega}(n)\\ &+\sum_{\sigma=1}^{\bar{\sigma}}\left(I_W\otimes B\tilde{K}_{\sigma,\theta(n)}\bar{F}_{\theta(n-\sigma)}\right)\bar{\omega}(n-\sigma)\\ &+\left(I_W\otimes B\bar{K}_{\theta(n)}\right)\bar{\Delta}_{\theta(n)}(n)\\ &+\sum_{\sigma=1}^{\bar{\sigma}}\left(I_W\otimes B\tilde{K}_{\sigma,\theta(n)}\right)\bar{\Delta}_{\theta(n-\sigma)}(n-\sigma) \quad (12)\end{aligned}$$

where

$$\begin{aligned}\bar{\omega}(n) &\triangleq (M^T\bar{L}\otimes I_{o_\omega})\omega(n),\\ \bar{\Delta}_{\theta(n)}(n) &\triangleq (M^T\bar{L}\otimes I_{o_y})\Delta_{\theta(n)}(n),\\ \tilde{\omega}(n) &\triangleq (M^T\otimes I_{o_\omega})\omega^a(n) + (M^TL_1^{-1}L_2\otimes I_{o_\omega})\omega^b(n).\end{aligned}$$

Remark 3: An auxiliary topological matrix is defined as $L \triangleq \mathcal{A} - \mathcal{D}$, whose first diagonal block of L is negative definite, which simplifies the representation of the closed-loop system dynamics by avoiding an explicit negative sign in the governing equations. Note that, the introduced matrix and the standard Laplacian matrix $L^* \triangleq \mathcal{D} - \mathcal{A}$ are mathematically equivalent up to a sign inversion. All spectral properties (including eigenvalue analysis and connectivity) remain consistent, with the eigenvalues of $L^* \triangleq \mathcal{D}-\mathcal{A}$ being non-negative and those of $L \triangleq \mathcal{A} - \mathcal{D}$ being non-positive. Crucially, the design process is unaffected by this sign convention.

Before presenting the main results, the following definition of boundedness is introduced.

Definition 3: [39] The closed-loop tracking error system (12) is said to be exponentially ultimately bounded if there are constants $\upsilon_1 > 0$, $1 > \upsilon_2 > 0$ and $\upsilon_3 > 0$ such that

$$\xi^T(n)\xi(n) \leq \upsilon_2^n\upsilon_1 + \upsilon_3$$

where υ_3 is referred to as the asymptotic upper bound (AUB) of the variable $\xi^T(n)\xi(n)$.

The aim of this paper is to design PID controllers that ensure the exponentially ultimate boundedness of system (12) while minimizing the AUB of the tracking error $\xi^T(n)\xi(n)$.

III. Main Results

Lemma 2: [35] For multi-rate measurement output (2), the resolution-introduced error defined in (4) satisfies

$$|\Delta_{i,q}^f(T_n)| \leq r_q^f, \quad |\Delta_{i,\iota}^s(t_n)| \leq r_\iota^s.$$

Lemma 3: [41] Given real matrices $X = X^T$, Y, Z and N with proper dimensions and satisfying $N^TN \leq I$, the following inequality

$$X + YNZ + Z^TN^TY^T < 0$$

holds if and only if there exists a scalar $\rho > 0$ such that

$$\begin{bmatrix} X & * & * \\ \rho Y^T & -\rho I & * \\ Z & 0 & -\rho I\end{bmatrix} < 0.$$

A. Boundedness Analysis

In the following theorem, a sufficient condition is presented to guarantee the boundedness of tracking error system (12).

Theorem 1: Consider the tracking error system (12) satisfying Assumptions 1–2. Let two scalars $\mu_1 > 0$, $1 > \mu_2 > 0$ and controller gains be given. Then, the closed-loop system (12) is exponentially ultimately bounded if, for $\nu = 1, 2, \cdots, 5$, $\bar{c} = 0, 1$, $c_\tau = 0, 1$ ($\tau = 0, 1, \cdots, \bar{\sigma}$), there exist three positive definite matrices $P_0 \in \mathbb{R}^{o_x\times o_x}$, $P_1 \in \mathbb{R}^{o_x\times o_x}$, $Q \in \mathbb{R}^{o_x\times o_x}$ and scalars $\alpha_\nu > 0$ such that

$$\Phi^T_{c_0,c_1,\cdots,c_{\bar{\sigma}}}\bar{P}_{\bar{c}}\Phi_{c_0,c_1,\cdots,c_{\bar{\sigma}}} + \Gamma_{c_0} < 0 \quad (13)$$

$$(1+\mu_1)^{m-1}(1-\mu_2) < 1 \quad (14)$$

where

$$\Phi^T_{c_0,c_1,\cdots,c_{\bar{\sigma}}} \triangleq \begin{bmatrix}\left(I_W\otimes A + \Theta\otimes B\bar{K}_{c_0}\bar{C}_{c_0}\right)^T\\ \tilde{B}^T_{c_1,\cdots,c_{\bar{\sigma}}}\\ \left(I_W\otimes B\bar{K}_{c_0}\bar{F}_{c_0}\right)^T\\ (I_W\otimes E)^T\\ \tilde{F}^T_{c_1,\cdots,c_{\bar{\sigma}}}\\ \left(I_W\otimes B\bar{K}_{c_0}\right)^T\\ \vec{K}^T\end{bmatrix},$$

This article has been accepted for publication in a future issue of this journal, but has not been fully edited. Content may change prior to final publication.
Citation information: DOI: 10.1109/JIOT.2025.3608094, EEE Internet of Things Journal

$$
\begin{aligned}
\tilde{B}_{c_1,\cdots,c_{\bar{\sigma}}} \triangleq &\big[\Theta\otimes B\tilde{K}_{1,c_0}\bar{C}_{c_1}\ \ \Theta\otimes B\tilde{K}_{2,c_0}\bar{C}_{c_2} \\
&\qquad\qquad \cdots\ \Theta\otimes B\tilde{K}_{\bar{\sigma},c_0}\bar{C}_{c_{\bar{\sigma}}}\big],\\
\tilde{F}_{c_1,\cdots,c_{\bar{\sigma}}} \triangleq &\big[I_W\otimes B\tilde{K}_{1,c_0}\bar{F}_{c_1}\ \ I_W\otimes B\tilde{K}_{2,c_0}\bar{F}_{c_2} \\
&\qquad\qquad \cdots\ I_W\otimes B\tilde{K}_{\bar{\sigma},c_0}\bar{F}_{c_{\bar{\sigma}}}\big],\\
\vec{K} \triangleq &\left[I_W\otimes B\tilde{K}_{1,c_0}\quad \cdots\quad I_W\otimes B\tilde{K}_{\bar{\sigma},c_0}\right],\\
\bar{P}_{c_0} \triangleq &\, I_W\otimes P_{c_0},\quad \bar{Q}\triangleq I_W\otimes Q,\\
\Gamma_{c_0} \triangleq &\,\mathrm{diag}\left\{\Gamma_{c_0}^{1,1},\Gamma_{c_0}^{2,2},\Gamma_{c_0}^{3,3},\Gamma_{c_0}^{4,4},\Gamma_{c_0}^{5,5},\Gamma_{c_0}^{6,6},\Gamma_{c_0}^{7,7}\right\},\\
\Gamma_0^{1,1} \triangleq & -(1+\mu_1)\bar{P}_0+\bar{\sigma}\bar{Q},\ \ \Gamma_{c_0}^{2,2}\triangleq-\tilde{Q},\\
\tilde{Q} \triangleq &\,\mathrm{diag}\left\{(1-\mu_2)\bar{Q},\cdots,(1-\mu_2)^{\bar{\sigma}}\bar{Q}\right\},\\
\Gamma_{c_0}^{3,3} \triangleq & -\alpha_1 I_W\otimes I_{o_\omega},\ \ \Gamma_{c_0}^{4,4}\triangleq-\alpha_2 I_W\otimes I_{o_\omega},\\
\Gamma_{c_0}^{5,5} \triangleq & -\alpha_3 I_W\otimes I_{\bar{\sigma}o_\omega},\Gamma_{c_0}^{6,6}\triangleq-\alpha_4 I_W\otimes I_{o_y},\\
\Gamma_{c_0}^{7,7} \triangleq & -\alpha_5 I_W\otimes I_{\bar{\sigma}o_y},\ \ \Gamma_1^{1,1}\triangleq-(1-\mu_2)\bar{P}_1+\bar{\sigma}\bar{Q}.
\end{aligned}
$$

Proof: Choose the following energy-like functional for boundedness analysis:

$$V(n)=V_1(n)+V_2(n) \tag{15}$$

where

$$
\begin{aligned}
V_1(n)&\triangleq\xi^T(n)\bar{P}_{\theta(n)}\xi(n),\\
V_2(n)&\triangleq\sum_{\sigma=1}^{\bar{\sigma}}\sum_{p=n-\sigma}^{n-1}(1-\mu_2)^{n-p-1}\xi^T(p)\bar{Q}\xi(p).
\end{aligned}
$$

Next, we discuss two different cases according to the sampling features.

Case 1: If $n\in\{t_\upsilon+1,t_\upsilon+2,\cdots,t_{\upsilon+1}-1\}$ $(\upsilon\in\mathbb{N})$, $\theta(n+1)=\bar{c}$ and $\theta(n-\sigma)=c_\sigma$, one has $n+1\in\{t_\upsilon+2,t_\upsilon+3,\cdots,t_{\upsilon+1}\}$ and $\theta(n)=0$. Then, the following difference is calculated:

$$
\begin{aligned}
&V_1(n+1)-(1+\mu_2)V(n)\\
&=\xi^T(n+1)\bar{P}_{\bar{c}}\xi(n+1)-(1+\mu_1)\xi^T(n)\bar{P}_{c_0}\xi(n)\\
&=\Bigg(\left(I_W\otimes A+\Theta\otimes B\bar{K}_{\theta(n)}\bar{C}_0\right)\xi(n)\\
&\quad+\sum_{\sigma=1}^{\bar{\sigma}}\left(\Theta\otimes B\tilde{K}_{\sigma,\theta(n)}\bar{C}_{\theta(n-\sigma)}\right)\xi(n-\sigma)\\
&\quad+\left(I_W\otimes B\bar{K}_{\theta(n)}\bar{F}_0\right)\bar{\omega}(n)+\left(I_W\otimes E\right)\tilde{\omega}(n)\\
&\quad+\sum_{\sigma=1}^{\bar{\sigma}}\left(I_W\otimes B\tilde{K}_{\sigma,\theta(n)}\bar{F}_{\theta(n-\sigma)}\right)\bar{\omega}(n-\sigma)\\
&\quad+\left(I_W\otimes B\bar{K}_{\theta(n)}\right)\bar{\Delta}_0(n)\\
&\quad+\sum_{\sigma=1}^{\bar{\sigma}}\left(I_W\otimes B\tilde{K}_{\sigma,\theta(n)}\right)\bar{\Delta}_{\theta(n-\sigma)}(n-\sigma)\Bigg)^T\bar{P}_{\bar{c}}\\
&\quad\times\Bigg(\left(I_W\otimes A+\Theta\otimes B\bar{K}_{\theta(n)}\bar{C}_0\right)\xi(n)\\
&\quad+\sum_{\sigma=1}^{\bar{\sigma}}\left(\Theta\otimes B\tilde{K}_{\sigma,\theta(n)}\bar{C}_{\theta(n-\sigma)}\right)\xi(n-\sigma)\\
&\quad+\left(I_W\otimes B\bar{K}_{\theta(n)}\bar{F}_0\right)\bar{\omega}(n)+\left(I_W\otimes E\right)\tilde{\omega}(n)\\
&\quad+\sum_{\sigma=1}^{\bar{\sigma}}\left(I_W\otimes B\tilde{K}_{\sigma,\theta(n)}\bar{F}_{\theta(n-\sigma)}\right)\bar{\omega}(n-\sigma)\\
&\quad+\left(I_W\otimes B\bar{K}_{\theta(n)}\right)\bar{\Delta}_0(n)\\
&\quad+\sum_{\sigma=1}^{\bar{\sigma}}\left(I_W\otimes B\tilde{K}_{\sigma,\theta(n)}\right)\bar{\Delta}_{\theta(n-\sigma)}(n-\sigma)\Bigg)\\
&\quad-(1+\mu_1)\xi^T(n)\bar{P}_{c_0}\xi(n)\\
&\triangleq\bar{\xi}^T(n)\left(\Phi_{0,c_1,\cdots,c_{\bar{\sigma}}}^T\bar{P}_{\bar{c}}\Phi_{0,c_1,\cdots,c_{\bar{\sigma}}}+\bar{\Gamma}_0\right)\bar{\xi}(n)
\end{aligned} \tag{16}
$$

where

$$
\begin{aligned}
\bar{\Gamma}_0&\triangleq\mathrm{diag}\left\{-(1+\mu_1)\bar{P}_0,0,0,0,0,0,0\right\},\\
\bar{\xi}(n)&\triangleq\left[\bar{\xi}_1^T(n)\quad\bar{\Delta}_{\theta(n)}^T(n)\quad\vec{\Delta}_{\theta(n)}^T(n)\right]^T,\\
\bar{\xi}_1(n)&\triangleq\left[\xi^T(n)\quad\tilde{\xi}^T(n)\quad\bar{\omega}^T(n)\quad\tilde{\omega}^T(n)\quad\vec{\omega}^T(n)\right]^T,\\
\tilde{\xi}^T(n)&\triangleq\left[\xi^T(n-1)\quad\xi^T(n-2)\quad\cdots\quad\xi^T(n-\bar{\sigma})\right]^T,\\
\vec{\omega}^T(n)&\triangleq\left[\bar{\omega}^T(n-1)\quad\bar{\omega}^T(n-2)\quad\cdots\quad\bar{\omega}^T(n-\bar{\sigma})\right]^T,\\
\vec{\Delta}_{\theta(n)}^T(n)&\triangleq\left[\bar{\Delta}_{\theta(n-1)}^T(n-1)\quad\cdots\quad\bar{\Delta}_{\theta(n-\bar{\sigma})}^T(n-\bar{\sigma})\right]^T.
\end{aligned}
$$

By calculating the difference of $V_2(n)$, one derives that

$$
\begin{aligned}
&V_2(n+1)-(1+\mu_1)V_2(n)\\
&\le V_2(n+1)-(1-\mu_2)V_2(n)\\
&=\sum_{\sigma=1}^{\bar{\sigma}}\Bigg(\sum_{p=n+1-\sigma}^{n}(1-\mu_2)^{n-p}\xi^T(p)\bar{Q}\xi(p)\\
&\qquad-\sum_{p=n-\sigma}^{n-1}(1-\mu_2)^{n-p}\xi^T(p)\bar{Q}\xi(p)\Bigg)\\
&=\xi^T(n)\bar{\sigma}\bar{Q}\xi(n)-\tilde{\xi}^T(n)\tilde{Q}\tilde{\xi}(n).
\end{aligned} \tag{17}
$$

In terms of the property of external noises, one deduces

$$\omega^T(n)\omega(n)\le\sum_{i=1}^{R}\hat{\omega}_i. \tag{18}$$

Then, one further has that

$$
\begin{aligned}
&\alpha_1\bar{\omega}^T(n)\bar{\omega}(n)\\
&=\alpha_1\omega^T(n)\left(M^T\bar{L}\otimes I_{o_\omega}\right)^T\left(M^T\bar{L}\otimes I_{o_\omega}\right)\omega(n)\\
&\triangleq\alpha_1\omega^T(n)\bar{M}\omega(n)\\
&\le\alpha_1\lambda_{\max}(\bar{M})\omega^T(n)\omega(n)\\
&\le\alpha_1\lambda_{\max}(\bar{M})\sum_{i=1}^{R}\hat{\omega}_i\triangleq\alpha_1\bar{\lambda}.
\end{aligned} \tag{19}
$$

Similarly, the following relation is established:

$$
\begin{aligned}
\alpha_2\tilde{\omega}^T(n)\tilde{\omega}(n)\le{}&2\alpha_2\lambda_{\max}(\vec{M})\sum_{i=1}^{W}\hat{\omega}_i\\
&+2\alpha_2\lambda_{\max}(\tilde{M})\sum_{i=W+1}^{R}\hat{\omega}_i\triangleq\tilde{\lambda},
\end{aligned} \tag{20}
$$

$$\alpha_3\vec{\omega}^T(n)\vec{\omega}(n)\le\alpha_3\bar{\sigma}\lambda_{\max}(\bar{M})\sum_{i=1}^{R}\hat{\omega}_i=\alpha_3\bar{\sigma}\bar{\lambda}. \tag{21}$$

where

$$
\begin{aligned}
\vec{M}&\triangleq(M^T\otimes I_{o_\omega})^T(M^T\otimes I_{o_\omega}),\\
\tilde{M}&\triangleq(M^TL_1^{-1}L_2\otimes I_{o_\omega})^T(M^TL_1^{-1}L_2\otimes I_{o_\omega}).
\end{aligned}
$$

This article has been accepted for publication in a future issue of this journal, but has not been fully edited. Content may change prior to final publication.
Citation information: DOI: 10.1109/JIOT.2025.3608094, EEE Internet of Things Journal

From Lemma 2, we know that

$$\Delta_0^T(n)\Delta_0(n) \leq \Delta_1^T(n)\Delta_1(n) \leq R\left(\sum_{q=1}^{o_{y_1}}\left(r_q^f\right)^2 + \sum_{\iota=1}^{o_{y_2}}\left(r_\iota^s\right)^2\right) \triangleq \bar{r}. \tag{22}$$

Then, one has that

$$\begin{aligned}&\alpha_4\bar{\Delta}_0^T(n)\bar{\Delta}_0(n)\\ &= \alpha_4\Delta_0^T(n)\left(M^T\bar{L}\otimes I_{o_y}\right)^T\left(M^T\bar{L}\otimes I_{o_y}\right)\Delta_0(n)\\ &\triangleq \alpha_4\Delta_0^T(n)\check{M}\Delta_0(n)\\ &\leq \alpha_4\Delta_1^T(n)\check{M}\Delta_1(n)\\ &\leq \alpha_4\lambda_{\max}\left(\check{M}\right)\bar{r}\end{aligned} \tag{23}$$

and

$$\begin{aligned}\alpha_5\vec{\Delta}_0^T(\theta(n))\vec{\Delta}_0(\theta(n)) &\leq \alpha_5\vec{\Delta}_1^T(\theta(n))\vec{\Delta}_1(\theta(n))\\ &\leq \alpha_5\bar{\sigma}\lambda_{\max}\left(\check{M}\right)\bar{r}.\end{aligned} \tag{24}$$

From (15) to (24), one concludes that

$$\begin{aligned}&V(n+1)-(1+\mu_1)V(n)\\ &\leq \bar{\xi}^T(n)\left(\Phi_{0,c_1,\cdots,c_{\bar{\sigma}}}^T\bar{P}_{\bar{c}}\Phi_{0,c_1,\cdots,c_{\bar{\sigma}}}+\Gamma_0\right)\bar{\xi}(n)+\varrho.\end{aligned} \tag{25}$$

where

$$\varrho \triangleq \alpha_1\bar{\lambda}+\alpha_3\bar{\sigma}\bar{\lambda}+\tilde{\lambda}+(\alpha_4+\alpha_5\bar{\sigma})\lambda_{\max}\left(\check{M}\right)\bar{r}.$$

It follows from (13) that

$$V(n+1)-(1+\mu_1)V(n) < \varrho, \tag{26}$$

which implies that, for any scalar $g>0$, the following can be calculated:

$$\begin{aligned}&g^{n+1}V(n+1)-g^nV(n)\\ &= g^{n+1}\left(V(n+1)-V(n)\right)+g^n(g-1)V(n)\\ &\leq g^{n+1}\left(\mu_1V(n)+\varrho\right)+g^n(g-1)V(n)\\ &= g^n(\mu_1g+g-1)V(n)+g^{n+1}\varrho.\end{aligned} \tag{27}$$

Choosing $\bar{g}\triangleq 1/(1+\mu_1)$, we infer from (27) that

$$\bar{g}^{n+1}V(n+1)-\bar{g}V(n) \leq \bar{g}^{n+1}\varrho. \tag{28}$$

Summarizing both sides of (28) from $n=t_\nu+1$ to $n=t_{\nu+1}-1$ leads to

$$\bar{g}^{t_{\nu+1}}V(t_{\nu+1})-\bar{g}^{t_\nu+1}V(t_\nu+1) \leq \frac{\bar{g}^{t_\nu+2}(1-\bar{g}^{m-1})}{1-\bar{g}}\varrho. \tag{29}$$

By considering $t_{\nu+1}-t_\nu = m(T_{\nu+1}-T_\nu)$, one has from (29) that

$$V(t_{\nu+1}) \leq \bar{g}^{1-m}V(t_\nu+1)+\frac{\bar{g}^{2-m}-\bar{g}}{1-\bar{g}}\varrho. \tag{30}$$

Case 2: If $n=t_\upsilon$ and $\theta(n-\sigma)=c_\sigma$, one has $n+1=t_\upsilon+1$, $\theta(n)=1$ and $\theta(n+1)=0$. By following a similar line along with **Case 1**, the following difference is calculated:

$$\begin{aligned}&V(n+1)-(1-\mu_2)V(n)\\ &\leq \bar{\xi}^T(n)\left(\Phi_{1,c_1,\cdots,c_{\bar{\sigma}}}^T\bar{P}_0\Phi_{1,c_1,\cdots,c_{\bar{\sigma}}}+\Gamma_1\right)\bar{\xi}(n)+\varrho.\end{aligned} \tag{31}$$

The condition (13) ensures that

$$V(n+1)-(1-\mu_2)V(n) \leq \varrho. \tag{32}$$

Thus, one can choose a scalar $\bar{d}=1/(1-\mu_2)$ such that

$$V(t_\nu+1) \leq \bar{d}^{-1}V(t_\nu)+\varrho. \tag{33}$$

By combining (30) with (33), the following holds:

$$\begin{aligned}V(t_{\nu+1}) &\leq \bar{g}^{1-m}\bar{d}^{-1}V(t_\nu)+\bar{g}^{1-m}\varrho+\frac{\bar{g}^{2-m}-\bar{g}}{1-\bar{g}}\varrho\\ &\triangleq \gamma V(t_\nu)+\bar{\varrho}.\end{aligned} \tag{34}$$

For $n\in\{t_\nu, t_\nu+1,\cdots,t_\nu+m-1\}$ and any scalar $\pi>0$, we have

$$\begin{aligned}&\pi^{\nu+1}V(t_{\nu+1})-\pi^\nu V(t_\nu)\\ &\triangleq \pi^\nu\big(\pi(V(t_{\nu+1})-V(t_\nu))+(\pi-1)V(t_\nu)\big)\\ &\leq \pi^\nu(\pi\gamma-1)V(t_\nu)+\pi^{\nu+1}\bar{\varrho}.\end{aligned} \tag{35}$$

Choosing $\bar{\pi}=1/\gamma$ yields

$$\bar{\pi}^{\nu+1}V(t_{\nu+1})-\bar{\pi}^\nu V(t_\nu) \leq \bar{\pi}^{\nu+1}\bar{\varrho}, \tag{36}$$

which further implies

$$V(t_\nu) \leq \bar{\pi}^{-\nu}V(0)+\frac{\bar{\pi}^{1-\nu}-\bar{\pi}}{1-\bar{\pi}}\bar{\varrho}. \tag{37}$$

The condition (14) is equivalent to $\bar{\pi}>1$. It is easy to see that, as $\nu\to+\infty$, $V(t_\nu)\to\frac{-\bar{\pi}\bar{\varrho}}{1-\bar{\pi}}<+\infty$. Thus, the dynamics of $V(t_\nu)$ is exponentially ultimately bounded.

Now, we are in a position to further discuss the boundedness of variable $V(n)$ for $\forall n\in\mathbb{N}$. For $n=t_\nu+1$ with $m=2$, we obtain from (33) and (37) that

$$V(n) \leq (1-\mu_2)\bar{\pi}^{-\nu}V(0)+(1-\mu_2)\frac{\bar{\pi}^{1-\nu}-\bar{\pi}}{1-\bar{\pi}}\bar{\varrho}+\varrho. \tag{38}$$

For $m\geq 3$ and $n\in\{t_\nu+2,\cdots,t_{\nu+1}-1\}$, it follows from (30) and (37) that

$$\begin{aligned}V(n) \leq\ &\bar{g}^{2-m}(1-\mu_2)\bar{\pi}^{-\nu}V(0)+\bar{g}^{2-m}(1-\mu_2)\frac{\bar{\pi}^{1-\nu}-\bar{\pi}}{1-\bar{\pi}}\bar{\varrho}\\ &+\bar{g}^{2-m}\varrho+\frac{\bar{g}^{3-m}-\bar{g}}{1-\bar{g}}\varrho.\end{aligned} \tag{39}$$

Thus, for $n\in\{t_\nu, t_\nu+1,\cdots,t_{\nu+1}-1\}$, one has

$$V(n) \leq \bar{\pi}^{-\nu}V(0)+\tilde{\varrho} \tag{40}$$

where

$$\tilde{\varrho} \triangleq \begin{cases}\frac{\bar{\pi}^{1-\nu}-\bar{\pi}}{1-\bar{\pi}}\bar{\varrho}+\varrho, & m=2\\ \bar{g}^{2-m}\frac{\bar{\pi}^{1-\nu}-\bar{\pi}}{1-\bar{\pi}}\bar{\varrho}+\left(\bar{g}^{2-m}+\frac{\bar{g}^{3-m}-\bar{g}}{1-\bar{g}}\right)\varrho, & m\geq 3.\end{cases}$$

According to Definition 3, the dynamics of $V(n)$ is exponentially ultimately bounded. The proof is now complete. ■

Citation information: DOI: 10.1109/JIOT.2025.3608094, EEE Internet of Things Journal

B. Controller Design

Theorem 2: Under Assumptions 1–2, we consider the tracking error system (12). Let two scalars $\mu_1 > 0$, $1 > \mu_2 > 0$ be given. Then, the closed-loop system (12) is exponentially ultimately bounded if, for $\nu = 1, 2, \cdots, 5$, $\bar{c} = 0, 1$, $c_\tau = 0, 1$ ($\tau = 0, 1, \cdots, \bar{\sigma}$), there exist five positive definite matrices P_0, P_1, X_0, X_1, $Q \in \mathbb{R}^{o_x \times o_x}$, matrices K_{P,c_0}, K_{I,c_0}, $K_{D,c_0} \in \mathbb{R}^{o_u \times o_y}$, and scalars $\alpha_\nu > 0$, $\rho_{c_0} > 0$ such that

$$\begin{bmatrix} \Xi_{\bar{c},c_0,\cdots,c_{\bar{\sigma}}} & * & * \\ \rho_{c_0}\lambda^{(2)} I & -\rho_{c_0} I & * \\ \Pi_{c_0,c_1,\cdots,c_{\bar{\sigma}}} & 0 & -\rho_{c_0} I \end{bmatrix} < 0 \tag{41}$$

$$(1+\mu_1)^{m-1}(1-\mu_2) < 1 \tag{42}$$

$$I_{o_x} \le P_{c_0} \tag{43}$$

$$P_{\bar{c}} X_{\bar{c}} = I_{o_x} \tag{44}$$

where

$$\begin{aligned}
\Xi_{\bar{c},c_0,\cdots,c_{\bar{\sigma}}} &\triangleq \begin{bmatrix} \tilde{\Gamma}_{c_0} & * \\ \bar{\Phi}_{c_0,c_1,\cdots,c_{\bar{\sigma}}} & -X_{\bar{c}} \end{bmatrix}, \\
\tilde{\Gamma}_{c_0} &\triangleq \mathrm{diag}\left\{\tilde{\Gamma}^{1,1}_{c_0}, \tilde{\Gamma}^{2,2}_{c_0}, \tilde{\Gamma}^{3,3}_{c_0}, \tilde{\Gamma}^{4,4}_{c_0}, \tilde{\Gamma}^{5,5}_{c_0}, \tilde{\Gamma}^{6,6}_{c_0}, \tilde{\Gamma}^{7,7}_{c_0}\right\}, \\
\tilde{\Gamma}^{1,1}_{0} &\triangleq -(1+\mu_1)P_0 + \bar{\sigma} Q,\ \tilde{\Gamma}^{2,2}_{c_0} \triangleq -\hat{Q}, \\
\hat{Q} &\triangleq \mathrm{diag}\left\{(1-\mu_2)Q, \cdots, (1-\mu_2)^{\bar{\sigma}} Q\right\}, \\
\tilde{\Gamma}^{3,3}_{c_0} &\triangleq -\alpha_1 I_{o_\omega},\ \tilde{\Gamma}^{4,4}_{c_0} \triangleq -\alpha_2 I_{o_\omega},\ \tilde{\Gamma}^{5,5}_{c_0} \triangleq -\alpha_3 I_{\bar{\sigma} o_\omega}, \\
\tilde{\Gamma}^{6,6}_{c_0} &\triangleq -\alpha_4 I_{o_y},\ \tilde{\Gamma}^{7,7}_{c_0} \triangleq -\alpha_5 I_{\bar{\sigma} o_y}, \\
\tilde{\Gamma}^{1,1}_{1} &\triangleq -(1-\mu_2)P_1 + \bar{\sigma} Q, \\
\bar{\Phi}^T_{c_0,c_1,\cdots,c_{\bar{\sigma}}} &\triangleq \begin{bmatrix} \left(A + \lambda^{(1)}(BK_{P,c_0} + BK_{D,c_0})\bar{C}_{c_0}\right)^T \\ \vec{B}^T_{c_1,\cdots,c_{\bar{\sigma}}} \\ \left(BK_{P,c_0}\bar{F}_{c_0} + BK_{D,c_0}\bar{F}_{c_0}\right)^T \\ E^T \\ \vec{F}^T_{c_1,\cdots,c_{\bar{\sigma}}} \\ \left(BK_{P,c_0} + BK_{D,c_0}\right)^T \\ \check{K}^T_{c_0} \end{bmatrix}, \\
\vec{B}_{c_0,\cdots,c_{\bar{\sigma}}} &\triangleq \left[\lambda^{(1)}(BK_{I,c_0} - BK_{D,c_0})\bar{C}_{c_1} \right. \\
&\qquad \left. \lambda^{(1)} BK_{I,c_0}\bar{C}_{c_2} \ \cdots \ \lambda^{(1)} BK_{I,c_0}\bar{C}_{c_{\bar{\sigma}}}\right], \\
\vec{F}_{c_0,\cdots,c_{\bar{\sigma}}} &\triangleq \left[(BK_{I,c_0} - BK_{D,c_0})\bar{F}_{c_1} \ BK_{I,c_0}\bar{F}_{c_2} \right. \\
&\qquad \left. \cdots \ BK_{I,c_0}\bar{F}_{c_{\bar{\sigma}}}\right], \\
\check{K}_{c_0} &\triangleq \left[(BK_{I,c_0} - BK_{D,c_0}) \ BK_{I,c_0} \right. \\
&\qquad \left. \cdots \ BK_{I,c_0}\right], \\
\Pi_{c_0,c_1,\cdots,c_{\bar{\sigma}}} &\triangleq \begin{bmatrix} 0 & 0 \\ \Pi^{(2,1)}_{c_0,c_1,\cdots,c_{\bar{\sigma}}} & 0 \end{bmatrix}, \\
\Pi^{(2,1)}_{c_0,c_1,\cdots,c_{\bar{\sigma}}} &\triangleq \left[(BK_{P,c_0} + BK_{D,c_0})\bar{C}_{c_0} \quad \tilde{C}_{c_1,\cdots,c_{\bar{\sigma}}} \quad 0\right], \\
\tilde{C}_{c_1,\cdots,c_{\bar{\sigma}}} &\triangleq \left[(BK_{I,c_0} - BK_{D,c_0})\bar{C}_{c_1} \ BK_{I,c_0}\bar{C}_{c_2} \right. \\
&\qquad \left. \cdots \ BK_{I,c_0}\bar{C}_{c_{\bar{\sigma}}}\right], \\
\lambda^{(1)} &\triangleq (\lambda_1 + \lambda_W)/2,\ \lambda^{(2)} \triangleq (\lambda_1 - \lambda_W)/2.
\end{aligned}$$

If the above conditions are satisfied, then the desired controller gains can be obtained directly from the matrix variables K_{P,c_0}, K_{I,c_0}, K_{D,c_0}. Furthermore, solving the following optimization problem yields the minimum AUB of the tracking error $\bar{x}^T(n)\bar{x}(n)$:

$$\min \sum_{\nu=1}^{5} \alpha_\nu \tag{45}$$

subject to (41)-(44).

Proof: It can be seen that the matrix in (13) is block diagonal. Thus, (13) can be guaranteed by

$$\left(\tilde{\Phi}^{(i)}_{c_0,c_1,\cdots,c_{\bar{\sigma}}}\right)^T P_{\bar{c}} \tilde{\Phi}^{(i)}_{c_0,c_1,\cdots,c_{\bar{\sigma}}} + \tilde{\Gamma}_{c_0} < 0 \tag{46}$$

where

$$\begin{aligned}
\tilde{\Phi}^{(i)T}_{c_0,c_1,\cdots,c_{\bar{\sigma}}} &\triangleq \begin{bmatrix} \left(A + \lambda_i B\bar{K}_{c_0}\bar{C}_{c_0}\right)^T \\ \left(\tilde{B}^{(i)}_{c_0,\cdots,c_{\bar{\sigma}}}\right)^T \\ \left(B\bar{K}_{c_0}\bar{F}_{c_0}\right)^T \\ E^T \\ \hat{F}^T_{c_0,\cdots,c_{\bar{\sigma}}} \\ \left(B\bar{K}_{c_0}\right)^T \\ \acute{K}^T_{c_0} \end{bmatrix}, \\
\tilde{B}^{(i)}_{c_0,\cdots,c_{\bar{\sigma}}} &\triangleq \left[\lambda_i B\tilde{K}_{1,c_0}\bar{C}_{c_1} \quad \cdots \quad \lambda_i B\tilde{K}_{\bar{\sigma},c_0}\bar{C}_{c_{\bar{\sigma}}}\right], \\
\hat{F}_{c_0,\cdots,c_{\bar{\sigma}}} &\triangleq \left[B\tilde{K}_{1,c_0}\bar{F}_{c_1} \quad \cdots \quad B\tilde{K}_{\bar{\sigma},c_0}\bar{F}_{c_{\bar{\sigma}}}\right], \\
\acute{K}_{c_0} &\triangleq \left[B\tilde{K}_{1,c_0} \quad B\tilde{K}_{2,c_0} \quad \cdots \quad B\tilde{K}_{\bar{\sigma},c_0}\right].
\end{aligned}$$

By utilizing condition (44) and the well-known Schur Complement lemma, (46) holds if and only if the following holds:

$$\begin{bmatrix} \tilde{\Gamma}_{c_0} & * \\ \tilde{\Phi}^{(i)}_{c_0,c_1,\cdots,c_{\bar{\sigma}}} & -X_{\bar{c}} \end{bmatrix} \triangleq \vec{\Gamma}^{(i)}_{\bar{c},c_0,\cdots,c_{\bar{\sigma}}} < 0. \tag{47}$$

Because $\lambda_1 \ge \lambda_2 \ge \cdots \ge \lambda_W$, there exist scalars $\varsigma_i \in [-1, 1]$ such that for $i \in \mathbb{F}$

$$\lambda_i = \lambda^{(1)} + \varsigma_i \lambda^{(2)}.$$

Thus, one obtains

$$\begin{aligned}
\vec{\Gamma}^{(i)}_{\bar{c},c_0,\cdots,c_{\bar{\sigma}}} = &\ \Xi_{\bar{c},c_0,\cdots,c_{\bar{\sigma}}} + \varsigma_i \lambda^{(2)} \Pi_{c_0,c_1,\cdots,c_{\bar{\sigma}}} \\
&+ \varsigma_i \lambda^{(2)} \Pi^T_{c_0,c_1,\cdots,c_{\bar{\sigma}}}.
\end{aligned} \tag{48}$$

According to Lemma 3, $\vec{\Gamma}^{(i)}_{c_0,\cdots,c_{\bar{\sigma}}} < 0$ can be guaranteed by the condition (41). Then, (13) holds, and together with (42), the closed-loop system (12) is exponentially ultimately bounded in terms of the results of Theorem 1.

From the definition of $\xi(n)$ in (12) and $M^T M = I$, one has $\bar{x}(n) = (M^T \otimes I_{o_x})^{-1}\xi(n)$, which together with (43), implies that

$$\begin{aligned}
\bar{x}^T(n)\bar{x}(n) &= \xi^T(n)\left((M^T \otimes I_{o_x})^{-1}\right)^T (M^T \otimes I_{o_x})^{-1}\xi(n) \\
&= \xi^T(n)\xi(n) \le V_1(n) \le V(n).
\end{aligned} \tag{49}$$

Then, from the result of boundedness analysis in (40), one can conclude that solving the optimization problem (45) can obtain the minimum value of the AUB of the tracking error $\bar{x}^T(n)\bar{x}(n)$. The proof is now complete. ■

Note that the minimization problem (45) is non-convex due to the equality constraint (44), which is difficult to solve using the linear inequality matrix (LMI) framework. To facilitate the calculation of PID controller gains, we utilize the cone

This article has been accepted for publication in a future issue of this journal, but has not been fully edited. Content may change prior to final publication.
Citation information: DOI: 10.1109/JIOT.2025.3608094, EEE Internet of Things Journal

complementarity linearization (CCL) technique [33] that can smoothly transform the original problem into a convex one subject to strict LMIs. Firstly, the following auxiliary matrix is defined:

$$\bar{X}_{\bar{c}} \triangleq \begin{bmatrix} P_{\bar{c}} & * \\ I_{o_x} & X_{\bar{c}} \end{bmatrix}.$$

Then, an iterative optimization method is given in Algorithm 1 for PID controller design.

Algorithm 1: PID Containment Control

Step 1. Choose $\mu_1 > 0$ and $\mu_2 > 0$ satisfying (43). Choose a series of sufficiently large initial value of $\alpha_\nu > 0$ ($\nu \in \{1, 2, 3, 4, 5\}$), such that there exist feasible solutions to (41), (43) and $\bar{X}_{\bar{c}} \geq 0$.

Step 2. Set $b = 0$. Obtain a set of initial solutions $\big(P_{c_0}^{(b)}, X_{c_0}^{(b)}, Q^{(b)}, K_{P,c_0}^{(b)}, K_{I,c_0}^{(b)}, K_{D,c_0}^{(b)}, \rho_{c_0}^{(b)}\big)$ by solving (41), (43) and $\bar{X}_{\bar{c}} \geq 0$.

Step 3. Solve min tr $\sum_{c_0=0}^{1}(P_{c_0}X_{c_0}^{(b)} + P_{c_0}^{(b)}X_{c_0})$ subject to (41), (43) and $\bar{X}_{\bar{c}} \geq 0$ with respect to the variable P_{c_0}, X_{c_0} and ρ_{c_0} to obtain an array of feasible solutions.

Step 4. Replace $-X_{\bar{c}}$ with $-P_{\bar{c}}^{-1}$ (obtained in *Step 3*) of the matrix in (41). Substitute the obtained gain matrices K_{P,c_0}, K_{I,c_0}, K_{D,c_0} into (41). If (41) is satisfied, then decrease α_ν ($\nu = 1, \cdots, 5$) to some extent and go to *Step 2*. If (41) is infeasible within the allowed maximum number of iterations, then exit. Otherwise, set $b = b+1$, $P_{c_0}^{(b)} = P_{c_0}$, $X_{c_0}^{(b)} = X_{c_0}$ and go to *Step 3*.

Remark 4: This paper focuses on MASs with an undirected communication topology. While undirected graphs entail higher implementation costs compared to their directed counterparts, they offer several fundamental advantages that justify their adoption. 1) The symmetry of the Laplacian matrix in undirected graphs substantially simplifies boundedness analysis. This structural property enables the derivation of scale-independent conditions, which are computationally efficient and amenable to distributed implementations; and 2) Undirected topologies exhibit enhanced resilience against link failures, ensuring reliable containment control in practical scenarios where communication uncertainties may arise. These merits collectively underscore the suitability of undirected graphs for the theoretical framework and performance guarantees pursued in this work.

Remark 5: This article is distinguished from existing literature by the following innovations. 1) This is the first work to examine the combined effects of multi-rate sampling and sensor resolution within a distributed control framework for general MASs. 2) Unlike previous studies assuming uniform sampling and ideal measurements, this work explicitly accounts for asynchronous data acquisition and sensor limitations, making the approach more practical. 3) A piecewise-based analysis and system transformation technique are introduced to handle time-varying system dynamics and simplify complex error system modeling. 4) The proposed approach improves controller flexibility while minimizing tracking errors, leading to more efficient containment control in practical MAS applications.

IV. Simulation Example

In this section, a simulation example is provided to verify the effectiveness of the proposed PID containment control method in addressing multi-rate measurements and sensor resolution effects.

A. System Parameters

Consider a class of linear MASs consisting of five moving vehicles, where the simple kinematic equation for the i-th vehicle is given as follows:

$$\dot{p}_i(t) = v_i(t), \quad \dot{v}_i(t) = a_i(t) \tag{50}$$

where $p_i(t)$, $v_i(t)$ and $a_i(t)$ are position, velocity and accelerated velocity respectively.

Choose $p_i(t)$, $v_i(t)$ as state variables and $a_i(t)$ as the control input. Then, by using the Euler discretization method with sampling time T and considering the external noises, we obtain dynamics in the form of (1) with the following parameters:

$$A = \begin{bmatrix} 1 & T \\ 0 & 1 \end{bmatrix}, \quad B = \begin{bmatrix} 0 \\ T \end{bmatrix}, \quad E = \begin{bmatrix} 0.2 \\ 0.05 \end{bmatrix}.$$

Each agent has two sensors with different sampling periods satisfying Assumption 2 with $m = 2$, meaning that the sampling period of the second sensor is twice that of the first sensor. The corresponding parameters are given by

$$C_1 = \begin{bmatrix} 1 & 0 \end{bmatrix}, \quad C_2 = \begin{bmatrix} 0 & 1 \end{bmatrix}, \quad F_1 = 0.2, \quad F_2 = 0.05.$$

B. Communication Topology

Assume that agents $1, 2, 3$ are followers and agents $4, 5$ are leaders. The agents communicate according to a fixed topology, illustrated in Fig. 1. The corresponding adjacency matrix is given by

$$\mathcal{A} = \begin{bmatrix} 0 & 2 & 0 & 2 & 0 \\ 2 & 0 & 1 & 0 & 0 \\ 0 & 1 & 0 & 0 & 2 \\ 0 & 0 & 0 & 0 & 0 \\ 0 & 0 & 0 & 0 & 0 \end{bmatrix}.$$

Then, the topological matrix is calculated as follows:

$$L = \begin{bmatrix} -4 & 2 & 0 & 2 & 0 \\ 2 & -3 & 1 & 0 & 0 \\ 0 & 1 & -3 & 0 & 2 \\ 0 & 0 & 0 & 0 & 0 \\ 0 & 0 & 0 & 0 & 0 \end{bmatrix}.$$

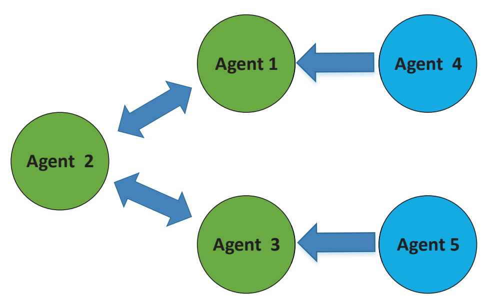

Fig. 1: Communication topology of the multi-agent system

For L_1, its eigenvalues are calculated as $\lambda_1 = -1.0968$, $\lambda_2 = -3.1939$ and -5.7093. The transformation matrix is obtained by

$$M = \begin{bmatrix} 0.7392 & -0.4271 & 0.5207 \\ -0.6318 & -0.1721 & 0.7558 \\ 0.2332 & 0.8877 & 0.3971 \end{bmatrix}.$$

This article has been accepted for publication in a future issue of this journal, but has not been fully edited. Content may change prior to final publication.
Citation information: DOI: 10.1109/JIOT.2025.3608094, EEE Internet of Things Journal

Then, one obtains $\lambda^{(1)} = -3.4030$ and $\lambda^{(2)} = 2.3062$ with the following relations:

$$\begin{aligned}\lambda_1 &= \lambda^{(1)} + 1 \times \lambda^{(2)}, \\ \lambda_2 &= \lambda^{(1)} + 0.0907 \times \lambda^{(2)}, \\ \lambda_3 &= \lambda^{(1)} - 1 \times \lambda^{(2)}.\end{aligned}$$

C. Simulation Setup

The sensor resolution is set to $r_1^f = r_1^s = 0.05$, and the system noise terms are assumed to be $\omega_1(n) = 0.12\sin(n)$, $\omega_2(n) = 0.11\sin(n)$, $\omega_3(n) = 0.13\sin(n)$, $\omega_4(n) = 0.12\cos(n)$, $\omega_5(n) = 0.12\cos(n)$. The initial states of agents are set as

$$x_1(0) = \begin{bmatrix} -10 \\ 8 \end{bmatrix}, \quad x_2(0) = \begin{bmatrix} -13 \\ 4 \end{bmatrix}, \quad x_3(0) = \begin{bmatrix} -6 \\ -2 \end{bmatrix},$$
$$x_4(0) = \begin{bmatrix} 8 \\ 2 \end{bmatrix}, \quad x_5(0) = \begin{bmatrix} -5 \\ 2 \end{bmatrix}.$$

The simulation is conducted for $n_{\max} = 500$ time steps. Set $T = 0.1$, the controller gains are calculated as follows:

$$\begin{aligned} K_{P,0} &= \begin{bmatrix} 0.0647 & 0 \end{bmatrix}, \quad K_{P,1} = \begin{bmatrix} 0.1837 & 0.8492 \end{bmatrix}, \\ K_{I,0} &= \begin{bmatrix} 0.0017 & 0 \end{bmatrix}, \quad K_{I,1} = \begin{bmatrix} 0.0025 & 0.0050 \end{bmatrix}, \\ K_{D,0} &= \begin{bmatrix} 0.0015 & 0 \end{bmatrix}, \quad K_{D,1} = \begin{bmatrix} 0.0017 & 0.0018 \end{bmatrix}. \end{aligned}$$

D. Simulation Results and Analysis

The simulation results are illustrated in Figs. 2–8.

- Figs. 2–3: State evolution of the open-loop system, showing instability.
- Figs. 4–5: State evolution of the closed-loop system, demonstrating stabilization under the proposed control method.
- Fig. 6 vs. Fig. 7: Comparison of the overall movement trajectory of the open-loop and closed-loop MASs, confirming the effectiveness of the containment strategy.
- Fig. 8: Tracking error $\bar{x}(n)$, verifying bounded error performance.

From the simulation results, the following conclusions can be drawn. 1) The original system is unstable, and there is no consensus behavior. 2) The proposed control method ensures that the three follower agents reach the convex hull formed by the two leaders despite multi-rate measurements and sensor resolution constraints. 3) The tracking error remains bounded, verifying the robustness and effectiveness of the proposed approach.

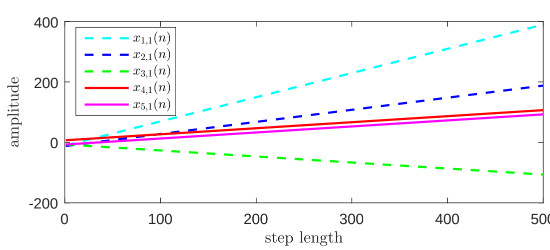

Fig. 2: The evolution of the first state variable of the open-loop MAS

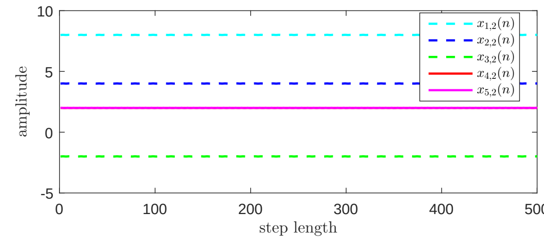

Fig. 3: The evolution of the second state variable of the open-loop MAS

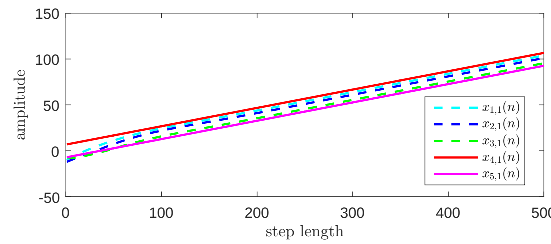

Fig. 4: The evolution of the first state variable of the closed-loop MAS

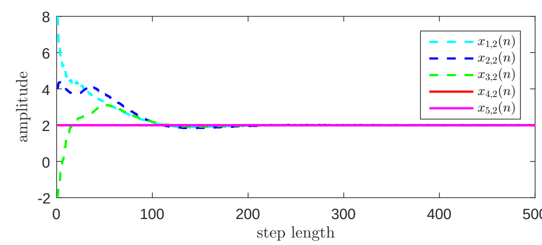

Fig. 5: The evolution of the second state variable of the closed-loop MAS

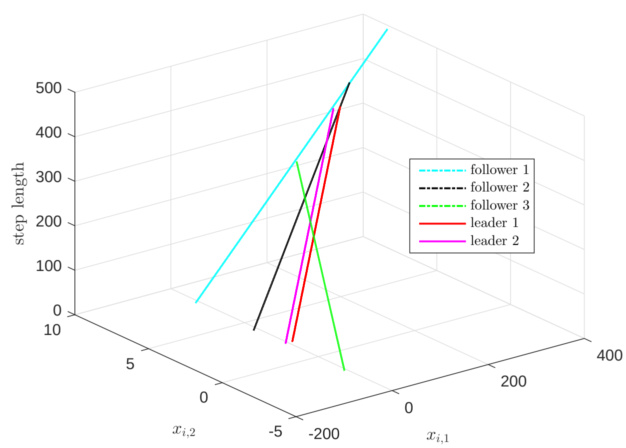

Fig. 6: The overall evolution of the open-loop MAS

E. Comparisons with Existing Results

To further analyze the impact of multi-rate sampling and sensor resolution, the accumulative tracking error is defined as:

$$e_{\text{sum}} \triangleq \sum_{n=1}^{n_{\max}} \sum_{\epsilon=1}^{6} |\bar{x}_\epsilon(n)|$$

This article has been accepted for publication in a future issue of this journal, but has not been fully edited. Content may change prior to final publication.
Citation information: DOI: 10.1109/JIOT.2025.3608094, EEE Internet of Things Journal

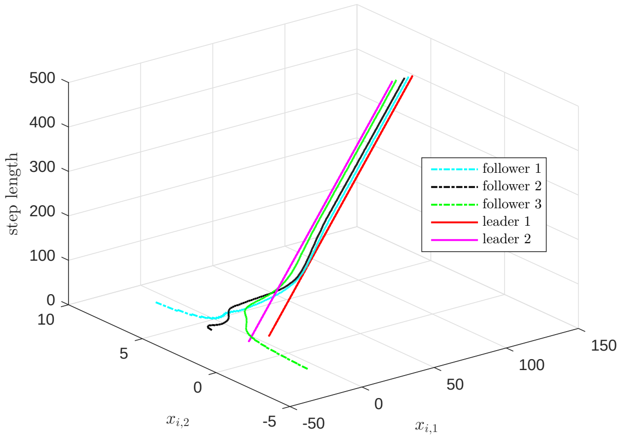

Fig. 7: The overall evolution of the closed-loop MAS

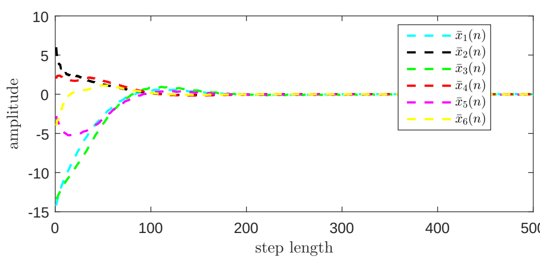

Fig. 8: The evolution of the tracking error system

Then, some comparison results are presented in Tables I and II which show the tracking performance of the proposed switching PID control and the traditional PID control with constant gains. Table I shows the calculated error under different levels of sensor resolution. Note that the larger value of r_1^f and r_1^s means the lower the resolution. It can be seen that a higher sensor resolution contributes to a better control performance which is consistent with the engineering fact. Table II displays the control performance under different sampling cases, where the larger value of m means the lower frequency that the measurement signals can be obtained for agents. It is observed that the system performance is improved by reducing the sampling periods of sensors which is reasonable. The results also indicate that the proposed containment PID controller exhibits enhanced performance relative to the traditional controller in the test cases. All simulation results validate the effectiveness of the proposed PID containment control strategy.

TABLE I: Accumulative tracking error under different levels of sensor resolution

Resolution level $r_1^f = r_1^s$	0.05	0.1	0.4	0.8
e_{sum} (10^3) in proposed PID	1.6866	1.6990	1.7921	2.3342
e_{sum} (10^3) in traditional PID	2.1235	2.3539	3.5153	3.7252

V. Conclusion

In this work, the containment control problem has been tackled for general linear MASs subject to multi-rate samplings and the constraint of sensor resolution. A comprehensive measurement model has been built that can not only feature the fast sampling and slow sampling, but also describe the error induced by resolution in a unified framework. A set of distributed PID controllers has been proposed for achieving the containment task. According to the sampling mechanism, the system has first been rewritten as a switching form and then transformed into a more concise one based on the topological matrix. In terms of the switching system theory and matrix inequality technique, sufficient conditions have been derived to check the system's boundedness. Furthermore, by using a modified CCL algorithm, the desired controller gains have been calculated and the parameters related to the performance have also been optimized. Finally, simulation examples together with some comparisons have been presented to validate the usefulness of the proposed approach. The future topics include the extension of the proposed method to nonlinear MASs with more complex sampling mechanisms (e.g., stochastic samplings and perturbed samplings) under directed communication topology.

TABLE II: Accumulative tracking error under different sampling cases

Sampling case	$m = 2$	$m = 3$	$m = 4$	$m = 5$
e_{sum} (10^3) in proposed PID	1.6866	2.5626	2.9659	3.3452
e_{sum} (10^3) in traditional PID	2.1235	3.4526	4.7881	4.9979

References

[1] M. Allen and H. K. Khalil, Performance recovery of a discrete-time MIMO nonlinear system using a fast observer, *Automatica*, vol. 161, art. no. 111485, Mar. 2024.

[2] H. A. P. Blom and E. A. Bloem, Bayesian tracking of two possibly unresolved maneuvering targets, *IEEE Transactions on Aerospace and Electronic Systems*, vol. 43, no. 2, pp. 612–627, Apr. 2007.

[3] H. A. P. Blom and E. A. Bloem, Exact Bayesian filter and joint IMM coupled PDA tracking of maneuvering targets from possibly missing and false measurements, *Automatica*, vol. 42, no. 1, pp. 127–135, Jan. 2006.

[4] R. Caballero-Águila, A. Hermoso-Carazo and J. Linares-Pérez, Networked fusion estimation with multiple uncertainties and time-correlated channel noise, *Information Fusion*, vol. 54, pp. 161–171, Feb. 2020.

[5] R. Caballero-Águila, A. Hermoso-Carazo and J. Linares-Pérez, Covariance-based fusion filtering for networked systems with random transmission delays and non-consecutive losses, *International Journal of General Systems*, vol. 46, no. 7, pp. 752–771, Jun. 2017.

[6] Y. Cao, D. Stuart, W. Ren and Z. Meng, Distributed containment control for multiple autonomous vehicles with double-integrator dynamics: Algorithms and experiments, *IEEE Transactions on Control Systems Technology*, vol. 19, no. 4, pp. 929–938, Jul. 2011.

[7] W. Chen, D. Ding, G. Wei, S. Zhang and Y. Li, Event-based containment control for multi-agent systems with packet dropouts, *International Journal of Systems Science*, vol. 49, no. 12, pp. 2658–2669, Jul. 2018.

[8] C. Li, Y. Liu, M. Gao and L. Sheng, Fault-tolerant formation consensus control for time-varying multi-agent systems with stochastic communication protocol, *International Journal of Network Dynamics and Intelligence*, vol. 3, no. 1, art. no. 100004, Mar. 2024.

[9] G.-F. Cui, L.-B. Wu and M. Wu, Adaptive event-triggered fault-tolerant control for leader-following consensus of multi-agent systems, *International Journal of Systems Science*, vol. 55, no. 15, pp. 3291–3303, Nov. 2024.

[10] F. Han, J. Liu, J. Li, J. Song, M. Wang and Y. Zhang, Consensus control for multi-rate multi-agent systems with fading measurements: the dynamic event-triggered case, *Systems Science & Control Engineering*, vol. 11, no. 1, art. no. 2158959, Jan. 2023.

[11] L. Zhao and B. Li, Adaptive fixed-time control for multiple switched coupled neural networks, *International Journal of Network Dynamics and Intelligence*, vol. 3, no. 3, art. no. 100018, Sept. 2024.

Citation information: DOI: 10.1109/JIOT.2025.3608094, EEE Internet of Things Journal

[12] M. Ghorbani, A. Tepljakov and E. Petlenkov, On robust stability of uncertain control systems with time delay: An approach based on the overlap of value sets, *IEEE Transactions on Automatic Control*, vol. 69, no. 9, pp. 6349–6356, Sept. 2024.

[13] W. Wang and M. Wang, Adaptive neural event-triggered output-feedback optimal tracking control for discrete-time pure-feedback nonlinear systems, *International Journal of Network Dynamics and Intelligence*, vol. 3, no. 2, art. no. 100010, Jun. 2024.

[14] M. Yuan and W. Qian, Adaptive output feedback tracking control for nonlinear systems with unknown growth rate, *International Journal of Network Dynamics and Intelligence*, vol. 3, no. 1, art. no. 100002, Mar. 2024.

[15] R. Sakthivel, A. Parivallal, O.-M. Kwon and S. Manickavalli, Observer-based leader-following cluster consensus for positive multi-agent systems with input time-varying delay, *International Journal of Systems Science*, vol. 55, no. 14, pp. 3017–3031, 2024.

[16] M. Ji, G. Ferrari-Trecate, M. Egerstedt and A. Buffa, Containment control in mobile networks, *IEEE Transactions on Automatic Control*, vol. 53, no. 8, pp. 1972–1975, Sept. 2008.

[17] F. Jia, F. Cao and X. He, Adaptive fault-tolerant tracking control for uncertain nonlinear systems with unknown control directions and limited resolution, *IEEE Transactions on Systems, Man, and Cybernetics: Systems*, vol. 53, no. 3, pp. 1813–1825, Mar. 2023.

[18] W. Diao, W. He, K. Liang and X. Tan, Adaptive impulsive consensus of nonlinear multi-agent systems via a distributed self-triggered strategy, *International Journal of Systems Science*, vol. 55, no. 11, pp. 2224–2238, 2024.

[19] H. Xiong, G. Chen, H. Ren, H. Li and R. Lu, Event-based model-free adaptive consensus control for multi-agent systems under intermittent attacks, *International Journal of Systems Science*, vol. 55, no. 10, pp. 2062–2076, 2024.

[20] A. T. Koru, A. Ramírez, S. B. Sarsilmaz, R. Sipahi, T. Yucelen and K. M. Dogan, Containment control of multi-human multi-agent systems under time delays, *IEEE Transactions on Systems, Man, and Cybernetics: Systems*, vol. 54, no. 6, pp. 3344-3356, Jun. 2024.

[21] N. Liu and W. Qian, Stability analysis of low-voltage direct current system with time-varying delay, *Systems Science & Control Engineering*, vol. 12, no. 1, art. no. 2293918, Jan. 2024.

[22] Y. Wang, C. Shen, J. Huang and H. Chen, Model-free adaptive control for unmanned surface vessels: a literature review, *Systems Science & Control Engineering*, vol. 12, no. 1, art. no. 2316170, Feb. 2024.

[23] F. Jin, L. Ma, C. Zhao and Q. Liu, State estimation in networked control systems with a real-time transport protocol, *Systems Science & Control Engineering*, vol. 12, no. 1, art. no. 2347885, May 2024.

[24] G.-P. Liu, Tracking control of multi-agent systems using a networked predictive PID tracking scheme, *IEEE/CAA Journal of Automatica Sinica*, vol. 10, no. 1, pp. 216–225, Jan. 2023.

[25] D. G. Lui, A. Petrillo and S. Santini, Leader tracking control for heterogeneous uncertain nonlinear multi-agent systems via a distributed robust adaptive PID strategy, *Nonlinear Dynamics*, vol. 108, no. 1, pp. 363–378, Mar. 2022.

[26] D. G. Lui, A. Petrillo and S. Santini, Bipartite tracking consensus for high-order heterogeneous uncertain nonlinear multi-agent systems with unknown leader dynamics via adaptive fully-distributed PID control, *IEEE Transactions on Network Science and Engineering*, vol. 10, no. 2, pp. 1131–1142, Mar./Apr. 2023.

[27] P. Gao, C. Jia and A. Zhou, Encryption-decryption-based state estimation for nonlinear complex networks subject to coupled perturbation, *Systems Science & Control Engineering*, vol. 12, no. 1, art. no. 2357796, Jul. 2024.

[28] Q. Ma and S. Xu, Consensusability of first-order multiagent systems under distributed PID controller with time delay, *IEEE Transactions on Neural Network and Learning Systems*, vol. 33, no. 12, pp. 7908–7912, Dec. 2022.

[29] F. Masiero, E. Sinibaldi, F. Clemente and C. Cipriani, Effects of sensor resolution and localization rate on the performance of a myokinetic control interface, *IEEE Sensors Journal*, vol. 21, no. 20, pp. 22603–22611, Oct. 2021.

[30] S. Morimoto, M. Sanada and Y. Takeda, High-performance current-sensorless drive for PMSM and SynRM with only low-resolution position sensor, *IEEE Transactions on Industry Applications*, vol. 39, no. 3, pp. 792–801, May/Jun. 2003.

[31] G.-R. Duan, Stabilisation of four types of underactuated systems: a FAS approach, *International Journal of Systems Science*, vol. 55, no. 12, pp. 2421–2441, 2024.

[32] H. Xiong, G. Chen, H. Ren, H. Li and R. Lu, Event-based model-free adaptive consensus control for multi-agent systems under intermittent attacks, *International Journal of Systems Science*, vol. 55, no. 10, pp. 2062–2076, 2024.

[33] J. Qiu, G. Feng and H. Gao, Asynchronous output-feedback control of networked nonlinear systems with multiple packet dropouts: T-S fuzzy affine model-based approach, *IEEE Transactions on Fuzzy Systems*, vol. 19, no. 6, pp. 1014–1030, Dec. 2011.

[34] A. Shariati and M. Tavakoli, A descriptor approach to robust leader-following output consensus of uncertain multi-agent systems with delay, *IEEE Transactions on Automatic Control*, vol. 62, no. 10, pp. 5310–5317, Oct. 2017.

[35] Y. Shen, Z. Wang, H. Liu, H. Dong and X. Yi, Recursive state estimation for multi-rate time-varying systems with multiplicative noises: Dealing with sensor resolutions, *International Journal of Robust and Nonlinear Control*, vol. 32, no. 10, pp. 6110–6126, Jul. 2022.

[36] C.-X. Shi and G.-H. Yang, Robust consensus control for a class of multi-agent systems via distributed PID algorithm and weighted edge dynamics, *Applied Mathematics and Computation*, vol. 316, pp. 73–88, Jan. 2018.

[37] H. Su, Y. Yang and Z. Gao, Semiglobal robust consensus of discrete-time MASs subject to input saturation and additive perturbations, *IEEE Transactions on Automatic Control*, vol. 68, no. 12, pp. 7997–8004, Dec. 2024.

[38] Y. Tang, X. Zhou, P. Li, J. Cao and J. Cheng, Sliding mode control for Markov jump singularly perturbed systems under piecewise homogeneous stochastic communication protocol, *IEEE Transactions on Cybernetics*, vol. 54, no. 7, pp. 4002–4013, Jul. 2024.

[39] Y. Wang, Z. Wang, L. Zou, L. Ma and H. Dong, Ultimately bounded PID control for T-S fuzzy systems under FlexRay communication protocol, *IEEE Transactions on Fuzzy Systems*, vol. 31, no. 12, pp. 4308–4320, Dec. 2023.

[40] Y. Xiao and W.-W. Che, Event-triggered fully distributed H_∞ containment control for MASs, *IEEE Transactions on Systems, Man, and Cybernetics: Systems*, vol. 54, no. 5, pp. 2676–2684, May 2024.

[41] L. Xie, Output feedback H_∞ control of systems with parameter uncertainty, *International Journal of Control*, vol. 63, no. 4, pp. 741–750, 1996.

[42] Y. Xu, H. Xiang, L. Yang, R. Lu and D. E. Quevedo, Optimal transmission strategy for multiple Markovian fading channels: Existence, structure, and approximation, *Automatica*, vol. 158, art. no. 111312, Dec. 2023.

[43] T. Yang, K. Bu, G. Chen, X. Xie and J. Xia, Fault-tolerant multi-rate sampled-data control for quadrotor UAV, *Nonlinear Dynamics*, vol. 112, no. 14, pp. 12253–12267, Jul. 2024.

[44] Y. Yang, S. Li, X. Ge and Q.-L. Han, Event-triggered cluster consensus of multi-agent systems via a modified genetic algorithm, *IEEE Transactions on Neural Networks and Learning Systems*, vol. 35, no. 5, pp. 6792–6805, May 2024.

[45] X. Yu, F. Yang, C. Zou and L. Qu, Stabilization parametric region of distributed PID controllers for general first-order multi-agent systems with time delay, *IEEE/CAA Journal of Automatica Sinica*, vol. 7, no. 6, pp. 1555–1564, Nov. 2020.

[46] H. Zhang, D. Yue, C. Dou, X. Xie and G. P. Hancke, Two-stage optimal operation strategy of isolated micro-grid with TSK fuzzy identification of supply security, *IEEE Transactions on Industrial Informatics*, vol. 16, no. 6, pp. 3731–3743, Jun. 2020.

[47] H. Zhang, D. Yue, C. Dou, X. Xie, K. Li and G. P. Hancke, Resilient optimal defensive strategy of TSK fuzzy-model-based Microgrids' system via a novel reinforcement learning approach, *IEEE Transactions on Neural Networks and Learning Systems*, vol. 34, no. 4, pp. 1921–1931, Apr. 2023.

[48] L. Zou, Z. Wang, H. Dong and Q.-L. Han, Moving horizon estimation with multirate measurements and correlated noises, *International Journal of Robust and Nonlinear Control*, vol. 30, no. 17, pp. 7429–7445, Nov. 2020.

Citation information: DOI: 10.1109/JIOT.2025.3608094, EEE Internet of Things Journal

Yezheng Wang received the B.Eng. degree in automation from the Qilu University of Technology, Jinan, China, in 2017, and the Ph.D. degree in control science and engineering from the Shandong University of Science and Technology, Qingdao, China, in 2024. He is currently a Lecturer with the School of Automation, Nanjing University of Information Science and Technology, Nanjing, China. From February 2023 to January 2024, he was a Visiting Ph.D. Student with the Department of Computer Science, Brunel University London, Uxbridge, U.K.

His current research interests include the control and filtering for T-S fuzzy systems.

Dr. Wang is a very active reviewer for many international journals.

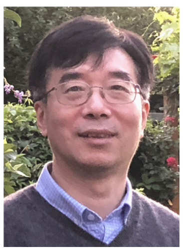

Zidong Wang (SM'03-F'14) received the B.Sc. degree in mathematics in 1986 from Suzhou University, Suzhou, China, and the M.Sc. degree in applied mathematics in 1990 and the Ph.D. degree in electrical engineering in 1994, both from Nanjing University of Science and Technology, Nanjing, China.

He is currently a Professor of Dynamical Systems and Computing in the Department of Computer Science, Brunel University London, Uxbridge, U.K. From 1990 to 2002, he held teaching and research appointments in universities in China, Germany and the U.K. Prof. Wang's research interests include dynamical systems, signal processing, bioinformatics, control theory and applications. He has published a number of papers in international journals. He is a holder of the Alexander von Humboldt Research Fellowship of Germany, the JSPS Research Fellowship of Japan, William Mong Visiting Research Fellowship of Hong Kong.

Prof. Wang serves (or has served) as the Editor-in-Chief for *International Journal of Systems Science*, the Editor-in-Chief for *Neurocomputing*, the Editor-in-Chief for *Systems Science & Control Engineering*, and an Associate Editor for 12 international journals including IEEE Transactions on Automatic Control, IEEE Transactions on Control Systems Technology, IEEE Transactions on Neural Networks, IEEE Transactions on Signal Processing, and IEEE Transactions on Systems, Man, and Cybernetics-Part C. He is a Member of the Academia Europaea, a Member of the European Academy of Sciences and Arts, an Academician of the International Academy for Systems and Cybernetic Sciences, a Fellow of the IEEE, a Fellow of the Royal Statistical Society and a member of program committee for many international conferences.

Lei Zou received the Ph.D. degree in control science and engineering in 2016 from Harbin Institute of Technology, Harbin, China.

He is currently a Professor with the College of Information Science and Technology, Donghua University, Shanghai, China. From October 2013 to October 2015, he was a Visiting Ph.D. Student with the Department of Computer Science, Brunel University London, Uxbridge, U.K. His research interests include control and filtering of networked systems, moving-horizon estimation, state estimation subject to outliers, and secure state estimation.

Prof. Zou serves (or has served) as an Associate Editor for *IEEE/CAA Journal of Automatica Sinica*, *Neurocomputing*, *International Journal of Systems Science*, and *International Journal of Control, Automation and Systems*, a Senior Member of *IEEE*, a Senior Member of *Chinese Association of Automation*, a Regular Reviewer of *Mathematical Reviews*, and a very active reviewer for many international journals.

Fan Wang received the Ph.D. degree in applied mathematics from Southeast University, Nanjing, China, in 2018.

She is currently a Professor with the School of Automation, Nanjing University of Information Science and Technology, Nanjing, China. From 2016 to 2018, she was a Visiting Ph.D. Student with the Department of Computer Science, Brunel University London, Uxbridge, U.K. From 2020 to 2021, she was a Post-Doctoral Fellow with the Department of Electrical and Computer Engineering, University of Macau, Macau, China. From 2022 to 2024, She was a Humboldt Research Fellow with the University of Duisburg-Essen, Duisburg, Germany. Her research interests include 2-D systems, networked control systems, recursive filtering, and optimal control.

Prof. Wang is a very active Reviewer for many international journals.

Hongli Dong received the Ph.D. degree in control science and engineering from the Harbin Institute of Technology, Harbin, China, in 2012.

From 2009 to 2010, she was a Research Assistant with the Department of Applied Mathematics, City University of Hong Kong, Hong Kong. From 2010 to 2011, she was a Research Assistant with the Department of Mechanical Engineering, The University of Hong Kong, Hong Kong. From 2011 to 2012, she was a Visiting Scholar with the Department of Information Systems and Computing, Brunel University London, Uxbridge, U.K. From 2012 to 2014, she was an Alexander von Humboldt Research Fellow with the University of Duisburg–Essen, Duisburg, Germany. She is currently a Professor with the Artificial Intelligence Energy Research Institute, Northeast Petroleum University, Daqing, China. She is also the Director of the Heilongjiang Provincial Key Laboratory of Networking and Intelligent Control, Daqing, China. Her current research interests include robust control and networked control systems.

Prof. Dong is a very active reviewer for many international journals.